Published in final edited form as:
Mol Cancer Ther. 2012 July ; 11(7): 1587–1597. doi:10.1158/1535-7163.MCT-11-1058.

Smoothened Antagonists Reverse Taxane Resistance in Ovarian Cancer

Adam D. Steg[1], **Ashwini A. Katre**[1], **Kerri S. Bevis**[1], **Angela Ziebarth**[1], **Zachary C. Dobbin**[1], **Monjri M. Shah**[1], **Ronald D. Alvarez**[1], and **Charles N. Landen**[1,*]

[1]Department of Obstetrics and Gynecology, University of Alabama at Birmingham, Birmingham, AL 35294

Abstract

The hedgehog (HH) pathway has been implicated in the formation and maintenance of a variety of malignancies, including ovarian cancer; however, it is unknown whether HH signaling is involved in ovarian cancer chemoresistance. The goal of this study was to determine the effects of antagonizing the HH receptor, Smoothened (Smo), on chemotherapy response in ovarian cancer. Expression of HH pathway members was assessed in 3 pairs of parental and chemotherapy-resistant ovarian cancer cell lines (A2780ip2/A2780cp20, SKOV3ip1/SKOV3TRip2, HeyA8/HeyA8MDR) using qPCR and Western blot. Cell lines were exposed to increasing concentrations of two different Smo antagonists (cyclopamine, LDE225) alone and in combination with carboplatin or paclitaxel. Selective knockdown of Smo, Gli1 or Gli2 was achieved using siRNA constructs. Cell viability was assessed by MTT assay. A2780cp20 and SKOV3TRip2 orthotopic xenografts were treated with vehicle, LDE225, paclitaxel or combination therapy. Chemoresistant cell lines demonstrated higher expression (>2-fold, $p<0.05$) of HH signaling components compared to their respective parental lines. Smo antagonists sensitized chemotherapy-resistant cell lines to paclitaxel, but not to carboplatin. LDE225 treatment also increased sensitivity of ALDH-positive cells to paclitaxel. A2780cp20 and SKOV3TRip2 xenografts treated with combined LDE225 and paclitaxel had significantly less tumor burden than those treated with vehicle or either agent alone. Increased taxane sensitivity appeared to be mediated by a decrease in P-glycoprotein (MDR1) expression. Selective knockdown of Smo, Gli1 or Gli2 all increased taxane sensitivity. Smo antagonists reverse taxane resistance in chemoresistant ovarian cancer models, suggesting combined anti-HH and chemotherapies could provide a useful therapeutic strategy for ovarian cancer.

Keywords

Smoothened; LDE225; paclitaxel; chemotherapy resistance; ovarian cancer

INTRODUCTION

Ovarian cancer is the leading cause of death from a gynecologic malignancy. Although ovarian cancer is among the most chemosensitive malignancies at the time of initial treatment (surgery and taxane/platinum-based chemotherapy), most patients will develop tumor recurrence and succumb to chemoresistant disease (1). Evaluation of multiple

*Corresponding Author: Charles N. Landen, Jr., MD, Assistant Professor, Department of Obstetrics and Gynecology, The University of Alabama at Birmingham, 1825 University Boulevard, 505 Shelby Building, Birmingham, AL 35294, Work: 205-934-0473, Fax: 205-934-0474, clanden@uab.edu.

Conflict of interest: No potential conflicts of interest were disclosed

chemotherapy agents in several combinations in the last 20 years has yielded modest improvements in progression-free survival, but no increase in durable cures. This clinical course suggests that a population of tumor cells has either inherent or acquired resistance to chemotherapy that allows survival with initial therapy and ultimately leads to recurrence. Targeting the cellular pathways involved in this resistance may provide new treatment modalities for ovarian cancer.

The Hedgehog (HH) pathway plays an important role in cell growth and differentiation during embryonic development (2). There are three known mammalian HH ligands – Sonic, Indian and Desert. These ligands are secreted peptides that bind to the transmembrane Patched (Ptch) receptor. In the absence of HH ligand, Ptch serves as a negative regulator of Smoothened (Smo), a G protein-coupled receptor. In the presence of HH ligand, Ptch repression of Smo is abolished, leading to downstream activation of the Gli family of transcription factors (Gli1, 2, 3). Gli transcription factors translocate from the cytoplasm to the nucleus, where they bind DNA and activate transcription of HH target genes, including *PTCH1* and *GLI1*, the expression of which are frequently measured to evaluate the presence or absence of HH pathway activity (3–4). Gli homologues have distinct, but overlapping functions; Gli1 serves only as a transcriptional activator, whereas Gli2 and Gli3 are capable of both activating and repressing HH gene transcription.

Recent reports have implicated HH signaling in multiple malignancies (5–6), including ovarian cancer (7–9), and suggest this pathway may be especially important in maintaining the subpopulation of cancer cells with stem cell properties (10–11) as well as conferring resistance to chemotherapies (12–13). Inhibition of the HH signaling pathway, therefore, has become a desirable therapeutic strategy for the treatment of various cancers. Cyclopamine, a steroidal alkaloid derived from the lily plant *Veratrum Californicum*, was the first compound identified that inactivates HH signaling by antagonizing Smo function (14–16). Since this discovery, pharmaceutical companies have synthesized more selective Smo antagonists, including NVP-LDE225 (17), which is currently being investigated in clinical trials (11).

The effects of Smo antagonists, both alone and in combination with chemotherapies, remains an active area of study in cancer research. Examination of combination effects is potentially important, given the hypothesized role of stem cell pathways in chemoresistance. However, the mechanisms by which HH inhibition might sensitize cells to chemotherapy, and whether such an approach would be effective in ovarian cancer, is not known. In our study, we sought to determine the effects of Smo antagonists on the viability of ovarian cancer cells, both alone and in combination with chemotherapy. We demonstrate that Smo antagonists have activity alone, but more dramatically can reverse taxane resistance in ovarian cancer, both *in vitro* and *in vivo*, through modulation of the multi-drug resistance mediator, P-glycoprotein (MDR1). These findings provide new insight into HH signaling, its contribution to an aggressive subpopulation of cells, and new opportunities for clinical development.

MATERIALS AND METHODS

Reagents and cell culture

Cyclopamine was purchased from Toronto Research Chemicals (North York, Ontario, Canada) and dissolved in 95% ethanol to create a 10 mM stock solution. NVP-LDE225 (LDE225) was kindly provided by Novartis Pharma AG (Basel, Switzerland) and dissolved in DMSO to create a 10 mM stock solution. The ovarian cancer cell lines A2780ip2, A2780cp20, HeyA8, HeyA8MDR, SKOV3ip1 and SKOV3TRip2 (18–23) were maintained in RPMI-1640 medium supplemented with 10% fetal bovine serum (Hyclone, Logan, UT). A2780cp20 (platinum- and taxane-resistant), HeyA8MDR (taxane-resistant) and

SKOV3TRip2 (taxane-resistant, a kind gift of Dr. Michael Seiden (24)) were generated by sequential exposure to increasing concentrations of chemotherapy (25). HeyA8MDR and SKOV3TRip2 were maintained with the addition of 150 ng/ml of paclitaxel. All cell lines were routinely screened for *Mycoplasma* species (GenProbe detection kit; Fisher, Itasca, IL) with experiments performed at 70–80% confluent cultures. Purity of cell lines was confirmed with STR genomic analysis, and only cells less than 20 passages from stocks were used in experiments.

RNA extraction and reverse transcription

Total RNA was isolated from ovarian cancer cell lines using Trizol reagent (Invitrogen, Carlsbad, CA) per manufacturer's instructions. RNA was then DNase treated and purified using the RNeasy Mini Kit (QIAGEN, Hilden, Germany). RNA was eluted in 50 μL of RNase-free water and stored at −80°C. The concentration of all RNA samples was quantified by spectrophotometric absorbance at 260/280 nm using an Eppendorf BioPhotometer plus (Hamburg, Germany). Prior to cDNA synthesis, all RNA samples were diluted to 20 ng/μL using RNase-free water. cDNA was prepared using the High Capacity cDNA Reverse Transcription Kit (Applied Biosystems, Foster City, CA). The resulting cDNA samples were analyzed using quantitative PCR.

Quantitative PCR

Primer and probe sets for *Desert HH* (Hs0036806_m1), *GLI1* (Hs00171790_m1), *GLI2* (Hs00257977_m1), *Indian HH* (Hs00745531_s1), *MDR1* (Hs00184500_m1), *PTCH1* (Hs00181117_m1), *SMO* (Hs00170665_m1), *Sonic HH* (Hs) and *RPLP0* (Hs99999902_m1; housekeeping gene) were obtained from Applied Biosystems and used according to manufacturer's instructions. PCR amplification was performed on an ABI Prism 7900HT sequence detection system and gene expression was calculated using the comparative C_T method as previously described (26). Briefly, this technique uses the formula $2^{-\Delta\Delta C_T}$ to calculate the expression of target genes normalized to a calibrator. The cycling threshold (C_T) indicates the cycle number at which the amount of amplified target reaches a fixed threshold. C_T values range from 0 to 40 (the latter representing the default upper limit PCR cycle number that defines failure to detect a signal).

Western blot analysis

Cultured cell lysates were collected in modified radioimmunoprecipitation assay (RIPA) lysis buffer with protease inhibitor cocktail (Roche, Manheim, Germany) and subjected to immunoblot analysis by standard techniques (25) using anti-Gli1 antibody (Cell Signaling Technology, Danvers, MA) at 1:1000 dilution overnight at 4°C; anti-Smo antibody (LifeSpan Biosciences, Seattle, WA) at 1:1000 dilution overnight at 4°C; or anti-β-actin antibody (AC-15, Sigma, St. Louis, MO) at 1:20,000 dilution for 1 hour at RT, which was used to monitor equal sample loading. After washing, blots were incubated with goat anti-rabbit (for Gli1 and Smo) or goat anti-mouse (for β-actin) secondary antibodies (Bio-Rad, Hercules, CA) conjugated with horseradish peroxidase. Visualization was performed by the enhanced chemiluminescence method (Pierce Thermo Scientific, Rockford, IL).

siRNA transfection

To examine downregulation of Smo, Gli1 or Gli2 individually with siRNA, cells were exposed to control siRNA (target sequence: 5'-UUCUCCGAACGUGUCACGU-3', Sigma), one of 2 tested Smo-targeting constructs (siRNA1: 5'-GAGGAGUCAUGACUCUGUUCUCCAU-3' or siRNA2: 5'-UGACCUCAAUGAGCCCUCAGCUGAU-3', Invitrogen), one of 2 tested Gli1-targeting constructs (siRNA1: 5'-CUACUGAUACUCUGGGAUA-3' or siRNA2: 5'-

GCAAAUAGGGCUUCACAUA-3', Sigma), or one of 2 tested Gli2-targeting constructs (siRNA1: 5'-GACAUGAGCUCCAUGCUCA-3' or siRNA2: 5'-CGAUUGACAUGCGACACCA-3', Sigma) at a 1:3 siRNA (μg) to Lipofectamine 2000 (μL) ratio. Lipofectamine and siRNA were incubated for 20 min at RT, added to cells in serum-free RPMI to incubate for up to 8 hours, followed by 10% FBS/RMPI thereafter. Transfected cells were grown at 37°C for 48–72 hours and then harvested for quantitative PCR or Western blot analysis.

Assessment of cell viability and cell cycle analysis

To a 96-well plate, 2,000 cells/well were exposed to increasing concentrations of cyclopamine or LDE225, alone or in combination with carboplatin or paclitaxel, in triplicate. Viability was assessed with 0.15% MTT (Sigma). For effects of siRNA-mediated downregulation on paclitaxel IC50, cells were first transfected with siRNA (5 μg) for 24 hours in 6-well plates, then trypsinized and re-plated at 2,000 cells per well, followed by addition of chemotherapy after attachment. IC50 of the agent of interest was determined by finding the dose at which the drug had 50% of its effect, calculated by the equation $[(OD450_{MAX}-OD450_{MIN})/2) + OD450_{MIN}]$. For cell cycle analysis, cells were treated with vehicle alone, paclitaxel alone, LDE225 alone or combined LDE225 and paclitaxel for 72 hours, trypsinized, and fixed in 100% ethanol overnight. Cells were then centrifuged, washed in PBS, and resuspended in PBS containing 0.1% Triton X-100 (v/v), 200 μg/mL DNase-free RNase A and 20 μg/mL propidium iodide (PI). PI fluorescence was assessed by flow cytometry and the percentage of cells in sub-G0, G0/G1, S and G2/M phases was calculated by the cell cycle analysis module for Flow Cytometry Analysis Software (FlowJo v.7.6.1, Ashland, OR).

ALDEFLUOR Assay

Active aldehyde dehydrogenase (ALDH) was identified with the ALDEFLUOR assay according to manufacturer's instructions (StemCell Technologies, Vancouver, BC). The ALDH-positive population was defined by cells with increased FITC signal absent in DEAB-treated cells, as previously decscribed (27). ALDEFLUOR-positive and -negative populations from SKOV3Trip2 cells were sorted with a FACS Aria II flow cytometer (BD Biosciences, San Jose, CA), and collected cells were seeded onto a 96-well plate at a concentration of 2,000 cells/well. Following overnight attachment, cells were then exposed to either DMSO or 5 μM LDE225, alone or in combination with increasing concentrations of paclitaxel. Viability was assessed with 0.15% MTT (Sigma).

Orthotopic ovarian cancer model

For orthotopic therapy experiments using ovarian cancer cell lines, female athymic nude mice (NCr-nu) were purchased from the National Cancer Institute (Frederick, MD) after Institution Animal Care and Use Committee approval of protocols, and cared for in accordance with guidelines of the American Association for Accreditation of Laboratory Animal Care. For all *in vivo* experiments, trypsinized cells were resuspended in 10% FBS-containing RPMI, washed with PBS, and suspended in serum-free HBSS at a concentration of 5×10^6 cells/mL, and 1×10^6 cells (A2780cp20 or SKOV3TRip2) were injected IP in 200 μL into 40 mice per experiment. After 1 week, mice (n = 10 per group) were randomized to treatment with 1) vehicle alone (0.5% methyl cellulose/0.5% Tween 80 in sterile water), 2) vehicle plus paclitaxel 75 μg), 3) LDE225 alone (60 mg/kg) or 4) combined LDE225 and paclitaxel. Vehicle and LDE225 were administered by gauvage once daily and paclitaxel was administered IP weekly. Mice were treated for 4 weeks (A2780cp20) or 6 weeks (SKOV3TRip2, which grow more slowly) before sacrifice and tumor collection. All tumors were excised and weighed in total.

Statistical analysis

Comparisons of gene expression, cell viability, PI fluorescence and mean tumor weight were analyzed using a two-tailed Student's t-test, if assumptions of data normality were met. Those represented by alternate distribution were examined using a nonparametric Mann-Whitney U test. Differences between groups were considered statistically significant at $p<0.05$. Error bars represent standard deviation unless otherwise stated. Number of mice per group (n=10) was chosen as directed by a power analysis to detect a 50% decrease in tumor growth with beta error of 0.2.

RESULTS

Expression of HH pathway members in chemosensitive and chemoresistant ovarian cancer cell lines

We first examined mRNA expression of HH ligands (Sonic (*SHH*), Indian (*IHH*), Desert (*DHH*)), receptors (*PTCH1*, *SMO*), and transcription factors (*GLI1*, *GLI2*) in 3 pairs of parental and chemoresistant ovarian cancer cell lines: A2780ip2 / A2780cp20 (20-fold increased cisplatin resistance and 10-fold increased taxane resistance); HeyA8 / HeyA8MDR (500-fold taxane resistant); and SKOV3ip1 / SKOV3TRip2 (1000-fold taxane resistant). As shown in Figure 1A, mRNA levels of *SHH* were significantly higher in A2780cp20 (17.4-fold, $p<0.05$) and SKOV3TRip2 (2.4-fold, $p<0.05$) cells compared to parental. *IHH* was also higher (3.5-fold, $p<0.05$) in SKOV3TRip2 cells with *DHH* expression remaining unchanged or decreased in chemoresistant cell lines compared to parental. mRNA levels of *PTCH1* were significantly higher (2.1-fold, $p<0.05$) in SKOV3TRip2 compared to parental SKOV3ip1 cells; however, no significant changes in *SMO* expression were observed between chemoresistant and chemosensitive cell lines (Figure 1B). Protein expression of Smo was confirmed in all cell lines tested and did not always correlate with expression at the mRNA level (Figure 1C). *GLI1* mRNA expression was significantly higher (2.0-fold, $p<0.05$) in A2780cp20 compared to parental A2780ip2 cells and *GLI2* mRNA expression was significantly higher (4.1-fold, $p<0.05$) in HeyA8MDR compared to parental HeyA8 cells, though at very low levels in both (Figure 1D). These results demonstrate that HH signaling is often higher in chemoresistant matched ovarian cancer cell lines.

Smo antagonists diminish cell viability and HH gene expression in ovarian cancer cell lines

Having observed Smo expression (both mRNA and protein) in both chemosensitive and chemoresistant ovarian cancer cell lines, we next examined response to the Smo antagonists cyclopamine and LDE225 among these cell lines. The chemical structure of LDE225 is shown in Figure 2A. As shown in Table 1, cyclopamine IC50s varied from 7.5 μM (A2780ip2) to 19 μM (SKOV3TRip2) and LDE225 IC50s varied from 7.5 μM (A2780cp20) to 24 μM (SKOV3ip1). Interestingly, chemoresistant cell lines were more sensitive (up to 2.25-fold, $p<0.05$) to LDE225 compared to their chemosensitive counterparts. Chemoresistant cell lines were also more sensitive to LDE225 than cyclopamine. In order to confirm that decreased cell viability was associated with diminished HH pathway activity, A2780cp20 cells were exposed to increasing concentrations of LDE225 (1, 5, 10 μM) for 72 hours and gene expression of HH target genes *PTCH1*, *GLI1* and *GLI2* was analyzed by qPCR. A dose-dependent decrease in the expression of all 3 genes was observed with a maximum reduction of 39%, 43% and 32% ($p<0.05$), respecitively, following exposure to 10 μM LDE225 (Figure 2B). Protein expression of the HH transcriptional activator Gli1 was also reduced in a dose-dependent manner following LDE225 treatment (Figure 2C). Taken together, these data demonstrate the efficacy and HH-specific acitivity of LDE225 in multiple chemoresistant cell lines.

Smo antagonism reverses taxane resistance in chemoresistant ovarian cancer cell lines both *in vitro* and *in vivo*

Having observed increased expression of HH signaling components and response to Smo antagonists in chemoresistant ovarian cancer cell lines, we sought to determine whether targeting the HH pathway could increase sensitivity to carboplatin and paclitaxel, chemotherapy agents most commonly used in the treatment of ovarian cancer. Neither cyclopamine nor LDE225 affected response to carboplatin among the chemoresistant cell lines examined (data not shown). However, as shown in Table 1, both Smo antagonists significantly increased the sensitivity of all three chemoresistant cell lines to paclitaxel (by up to 27- and 20-fold, respectively; $p<0.05$). Increased sensitivity to paclitaxel following combination with cyclopamine or LDE225 even occurred at low doses that were not effective alone (5 μM cyclopamine, Figure 3A; and 1 μM LDE225, Figure 3B). To determine the mechanism by which Smo antagonism combined with paclitaxel affects cell growth, we performed cell cycle analysis on A2780cp20 cells that were treated with DMSO alone (vehicle control), paclitaxel alone (30 nM), LDE225 alone (5 μM) or combined paclitaxel and LDE225 for 72 hours. As shown in Figure 3C, combination treatment resulted in a greater accumulation of cells in the sub-G0/apoptotic, S and G2/M phases compared to control or either treatment alone. These data suggest that LDE225 enhances cell cycle arrest and cell death induced by the microtubule-stabilizing effects of paclitaxel.

To determine if LDE225 can similarly reverse taxane resistance *in vivo*, an orthotopic mouse model using chemoresistant cell lines was employed. Nude mice were injected intraperitoneally with either A2780cp20 or SKOV3TRip2 cells and randomized to four treatment groups: 1) vehicle alone; 2) paclitaxel alone (75 μg weekly); 3) LDE225 alone (60 mg/kg daily); or 4) combined paclitaxel and LDE225. When control mice started to become moribund with tumor burden, all mice were sacrificed and total tumor weights recorded. In the A2780cp20 model (Figure 3D), there was no significant reduction in tumor growth with either paclitaxel or LDE225 alone. However, the combination of paclitaxel and LDE225 resulted in significantly reduced tumor weight, by 65.7% compared to vehicle alone ($p=0.028$). This represented a 60.7% reduction compared to paclitaxel alone ($p=0.014$) and a 68% reduction compared to LDE225 alone ($p=0.010$), again demonstrating synergy of paclitaxel and LDE225. Similar results were observed in SKOV3TRip2 xenografts (Figure 3E). Neither paclitaxel nor LDE225 alone had a statistically significant impact on tumor growth, whereas combination treatment significantly reduced tumor weight, by 70.4% compared to vehicle alone ($p=0.015$). This represented a 56.6% reduction compared to paclitaxel alone ($p=0.18$) and a 58.8% reduction compared to LDE225 alone ($p=0.13$), though neither was statistically significant.

LDE225 sensitizes chemoresistant ovarian cancer cells to paclitaxel by downregulating MDR1 expression and sensitizes both ALDH-negative and -positive ovarian cancer cells to paclitaxel

The primary mediator of taxane resistance in general, and in the chemoresistant cell lines examined in this study (27), is expression of the drug efflux protein, P-glycoprotein (ABCB1/MDR1). To identify the mechanism underlying taxane sensitization following Smo antagonism, we next examined whether LDE225 could modulate *MDR1* gene expression. In A2780cp20 cells exposed to LDE225 alone, paclitaxel alone and combined LDE225 + paclitaxel for 72 hours, it was observed that LDE225 decreased *MDR1* expression (by up to 49.2%, $p<0.05$), whereas paclitaxel actually led to a compensatory *increase* in *MDR1* expression (2.88-fold, $p<0.05$) compared to vehicle control (Figure 4A). This compensatory increase in *MDR1* was alleviated by LDE225 in a dose-dependent manner (up to a 59.9% decrease, $p<0.05$), demonstrating that this compound increases sensitivity to paclitaxel, at least in part, by downregulating *MDR1*. Similar results were observed in SKOV3TRip2

cells (Figure 4B); LDE225 decreased *MDR1* expression both alone (by up to 36.4%, $p<0.05$ compared to vehicle control) and in combination with paclitaxel (by up to 50.8%, $p<0.05$ compared to paclitaxel alone). In this cell line, a compensatory increase in *MDR1* was not observed with paclitaxel alone, likely because *MDR1* is already expressed at extremely high levels (140-fold more than in A2780cp20) in this 1000-fold taxane-resistant cell line (27). To determine if similar modulation of *MDR1* occurs *in vivo*, RNA isolated from A2780cp20 tumors (from Figure 3D) was examined. In agreement with the *in vitro* data, LDE225 alone significantly reduced *MDR1* expression (by 35.2%, $p<0.05$) and paclitaxel alone significantly increased *MDR1* expression (2.55-fold, $p<0.05$) compared to vehicle control (Figure 4C). In addition, combination treatment significantly reduced *MDR1* expression compared to paclitaxel alone (by 48.8%, $p<0.05$), blunting this compensatory rise.

In addition to our examination of MDR1 expression following LDE225 treatment, we also examined βIII-tubulin and stathmin, proteins that have been associated with microtubule regulation and resistance to taxanes (28). It was found that neither of these proteins was affected by LDE225 treatment *in vitro* (as determined by Western blot, data not shown). Taken together, these data support a mechanism whereby LDE225 causes the downregulation of *MDR1* expression, which then leads to increased uptake of paclitaxel within chemoresistant cells, rather than potentiating the microtubule stabilizing effect of this compound.

We have previously shown that ALDH activity is associated with enhanced tumorigenicity and chemoresistance in ovarian cancer, and may define one of potentially many cancer cell populations with stem cell-like features (27, 29). To determine whether cancer stem cells (CSCs) might play a role in taxane sensitization following LDE225 treatment, we collected ALDH-negative and -positive cell populations from the SKOV3TRip2 cell line, and exposed them to combined LDE225 and paclitaxel. As shown in Figure 4D, it was found that ALDH-negative and -positive SKOV3TRip2 cells demonstrated a similar decrease in viability following LDE225 treatment alone (21.4% versus 16.8%, respectively), compared to DMSO control. In addition, sensitivity to paclitaxel (as determined by IC50) was similarly increased following combination treatment in ALDH-negative and -positive cells (5.1-fold versus 4.0-fold change in IC50, respectively). These results indicate that the more tumorigenic ALDH-positive cells are just as susceptible to LDE225 treatment as ALDH-negative cells, and that HH inhibition can sensitize both populations to taxane therapy. Whether other putative CSC populations such as CD133, CD44, and the side population, with which there is some (but not complete) crossover with the ALDH population (30), can also be sensitized to taxanes will be the subject of future investigations.

Knockdown of Smo diminishes HH pathway activity, reduces viability and reverses taxane resistance in ovarian cancer cells

To determine whether LDE225 reverses taxane resistance through inhibition of Smo alone or off-target effects, we selectively targeted HH pathway members using siRNAs and observed effects on HH pathway activity and paclitaxel response. As shown in Figure 5A, knockdown of Smo was achieved both at the mRNA and protein level. As expected, this downregulation led to a significant decrease in HH target genes *PTCH1* (66.6%, $p<0.01$), *GLI1* (86.5%, $p<0.01$) and *GLI2* (62.0%, $p<0.01$). Individual knockdown of HH mediators Smo, Gli1 or Gli2 using 2 distinct siRNA constructs for each gene led to increased sensitivity to paclitaxel (Figure 5B–D). In particular, Smo knockdown decreased paclitaxel IC50 by up to 11.7-fold; Gli1 knockdown, up to 3.5-fold; and Gli2 knockdown, up to 5.9-fold. In agreement with cyclopamine and LDE225 biological effects, knockdown of Smo, Gli1 or Gli2 alone significantly decreased cell viability (by up to 73.5%, 57.6% and 26.5%, respectively, $p<0.01$) compared to control siRNA. Collectively, these data suggest that HH signaling promotes ovarian cancer cell survival and mediates taxane resistance.

DISCUSSION

In the current study, we found that HH pathway signaling components are overexpressed in chemoresistant ovarian cancer cells. Moreover, targeting the HH pathway decreased ovarian cancer cell viability and sensitized chemoresistant ovarian cancer cells to paclitaxel therapy through decreased *MDR1* expression. The participation of HH signaling in ovarian cancer cell survival and chemotherapy resistance makes it an attractive target for therapy, especially since most ovarian cancer patients develop tumor recurrence and succumb to chemoresistant disease.

Currently, it has not been shown what role HH signaling might play in mediating ovarian cancer chemoresistance, a persistent obstacle in the treatment of this disease. While the clinical behavior of ovarian cancer suggests that most cancer cells are initially sensitive to chemotherapy, they subsequently either develop resistance or contain a population of cells that are inherently resistant. The latter hypothesis is consistent with what has become known as tumor initiating cells or cancer stem cells (CSCs). These CSCs are commonly believed to have enhanced tumorigenicity, differentiation capacity and resistance to chemotherapy in comparison to non-CSCs. It is because of these features that CSCs have been examined for molecular pathways and markers that could be targeted for therapeutic purposes. Recent studies have suggested that developmental pathways, including HH, play important roles in the maintenance of CSCs (10–11) and that inhibiting these pathways may provide enhanced chemosensitivity when combined with traditional chemotherapies. In our study, we sought to define a role for HH signaling in ovarian cancer chemoresistance. Both *in vitro* and *in vivo*, we observed significant sensitization to paclitaxel following Smo antagonism (LDE225) in taxane-resistant ovarian cancer cells. This sensitization was also present in ALDH-positive cells, a subpopulation of cancer cells with enhanced tumorigenicity and chemoresistance. The mechanism underlying this sensitization appears to involve downregulation of P-glycoprotein (ABCB1/MDR1), a well-characterized mediator of multi-drug resistance. By downregulating *MDR1* expression, uptake of paclitaxel by cancer cells would be increased, resulting in a greater response to the chemotherapeutic agent. This mechanism would explain why Smo antagonists did not sensitize chemoresistant cells to carboplatin, since this compound is not a substrate for the P-glycoprotein drug efflux pump. In addition, this model of HH inhibition and chemosensitization agrees with a previous study performed by Sims-Mourtada et al., in which it was demonstrated that cyclopamine sensitized prostate cancer cells to a variety of chemotherapy agents *in vitro* (including the taxane docetaxel), through modulation of MDR1 expression (12). The observation that Smo antagonism did not sensitize cells to platinum therapy highlights the specificity of this effect.

Previous studies have demonstrated aberrant expression of the HH pathway in primary specimens of ovarian cancer compared to normal ovarian epithelium (7–9), including a study that found elevated Gli1 expression is associated with decreased survival (9). These studies have also demonstrated decreased ovarian cancer cell growth/viability following treatment with the Smo antagonist cyclopamine, results that our study supports. We have previously shown that *GLI1* and *GLI2* mRNA levels were significantly higher in cancer cells isolated from persistent/chemoresistant tumors compared to those isolated from matched primary tumors (29). Smoothened expression was also increased (3.7-fold) in persistent tumors; however, this increase was not statistically significant. Patients from whom persistent tumors were obtained had failed both taxane and platinum chemotherapies, making it difficult to determine whether this increase in hedgehog pathway genes is a taxane-specific effect. The *in vitro* data presented in this study, however, would suggest that Smoothened, as well as Gli1 and Gli2, are associated with taxane resistance. In our initial experiments examining the effects of targeting HH alone, either with Smo antagonists or

RNAi, ovarian cancer cell viability was significantly decreased *in vitro*, indicating that the HH pathway is important for ovarian cancer survival. However, this effect did not seem to translate to our xenograft models, in which the Smo antagonist LDE225 had no significant impact on tumor growth when used alone, even in models with relatively high Gli1 expression. These findings suggest that survival pathways are activated in the murine tumor microenvironment that allows resistance to HH antagonist monotherapy. Given the recognized importance of crosstalk between the tumor stromal cells and malignant cells in the HH pathway (6), and the failure of this model to target both murine and human compartments, more efficacy may be noted with monotherapy in humans.

Collectively, the data presented in this study demonstrate that increased expression of HH signaling components is associated with taxane resistance, which can be overcome by targeting multiple effectors of the HH signaling pathway. With the ability to identify subsets of cancer patients with HH pathway overexpression, antagonism of HH signaling in combination with taxane therapy could ultimately provide a useful therapeutic strategy for recurrent, chemoresistant ovarian cancer.

Acknowledgments

NVP-LDE225 was kindly provided by Novartis Pharma AG (Basel, Switzerland).

GRANT SUPPORT

Funding support provided by the University of Alabama at Birmingham Center for Clinical and Translational Science (5UL1RR025777, C.N. Landen), the Reproductive Scientist Development Program through the Ovarian Cancer Research Fund and the National Institutes of Health (K12 HD00849, C.N. Landen), the Gynecologic Cancer Foundation and the Department of Defense Ovarian Cancer Research Academy (OC093443, C.N. Landen).

Abbreviations

HH	Hedgehog
Smo	Smoothened
LDE225	NVP-LDE225

REFERENCES

1. Bhoola S, Hoskins WJ. Diagnosis and management of epithelial ovarian cancer. Obstet Gynecol. 2006; 107:1399–1410. [PubMed: 16738170]
2. Hooper JE, Scott MP. Communicating with Hedgehogs. Nature reviews. 2005; 6:306–317.
3. Ruiz i Altaba A, Mas C, Stecca B. The Gli code: an information nexus regulating cell fate, stemness and cancer. Trends Cell Biol. 2007; 17:438–447. [PubMed: 17845852]
4. Stecca B, Ruiz IAA. Context-dependent regulation of the GLI code in cancer by HEDGEHOG and non-HEDGEHOG signals. J Mol Cell Biol. 2010; 2:84–95. [PubMed: 20083481]
5. Pasca di Magliano M, Hebrok M. Hedgehog signalling in cancer formation and maintenance. Nat Rev Cancer. 2003; 3:903–911. [PubMed: 14737121]
6. Theunissen JW, de Sauvage FJ. Paracrine Hedgehog signaling in cancer. Cancer Res. 2009; 69:6007–6010. [PubMed: 19638582]
7. Chen X, Horiuchi A, Kikuchi N, Osada R, Yoshida J, Shiozawa T, et al. Hedgehog signal pathway is activated in ovarian carcinomas, correlating with cell proliferation: it's inhibition leads to growth suppression and apoptosis. Cancer Sci. 2007; 98:68–76. [PubMed: 17083567]
8. Bhattacharya R, Kwon J, Ali B, Wang E, Patra S, Shridhar V, et al. Role of hedgehog signaling in ovarian cancer. Clin Cancer Res. 2008; 14:7659–7666. [PubMed: 19047091]

9. Liao X, Siu MK, Au CW, Wong ES, Chan HY, Ip PP, et al. Aberrant activation of hedgehog signaling pathway in ovarian cancers: effect on prognosis, cell invasion and differentiation. Carcinogenesis. 2009; 30:131–140. [PubMed: 19028702]
10. Ruiz i Altaba A. Therapeutic inhibition of Hedgehog-GLI signaling in cancer: epithelial, stromal, or stem cell targets? Cancer Cell. 2008; 14:281–283. [PubMed: 18835029]
11. Merchant AA, Matsui W. Targeting Hedgehog--a cancer stem cell pathway. Clin Cancer Res. 2010; 16:3130–3140. [PubMed: 20530699]
12. Sims-Mourtada J, Izzo JG, Ajani J, Chao KS. Sonic Hedgehog promotes multiple drug resistance by regulation of drug transport. Oncogene. 2007; 26:5674–5679. [PubMed: 17353904]
13. Singh RR, Kunkalla K, Qu C, Schlette E, Neelapu SS, Samaniego F, et al. ABCG2 is a direct transcriptional target of hedgehog signaling and involved in stroma-induced drug tolerance in diffuse large B-cell lymphoma. Oncogene. 2011
14. Binns W, James LF, Shupe JL, Everett G. A Congenital Cyclopian-Type Malformation in Lambs Induced by Maternal Ingestion of a Range Plant, Veratrum Californicum. Am J Vet Res. 1963; 24:1164–1175. [PubMed: 14081451]
15. Cooper MK, Porter JA, Young KE, Beachy PA. Teratogen-mediated inhibition of target tissue response to Shh signaling. Science (New York, NY. 1998; 280:1603–1607.
16. Chen JK, Taipale J, Cooper MK, Beachy PA. Inhibition of Hedgehog signaling by direct binding of cyclopamine to Smoothened. Genes & development. 2002; 16:2743–2748. [PubMed: 12414725]
17. Buonamici S, Williams J, Morrissey M, Wang A, Guo R, Vattay A, et al. Interfering with resistance to smoothened antagonists by inhibition of the PI3K pathway in medulloblastoma. Sci Transl Med. 2010; 2:51ra70.
18. Louie KG, Behrens BC, Kinsella TJ, Hamilton TC, Grotzinger KR, McKoy WM, et al. Radiation survival parameters of antineoplastic drug-sensitive and -resistant human ovarian cancer cell lines and their modification by buthionine sulfoximine. Cancer Res. 1985; 45:2110–2115. [PubMed: 3986765]
19. Landen CN, Kim TJ, Lin YG, Merritt WM, Kamat AA, Han LY, et al. Tumor-selective response to antibody-mediated targeting of alphavbeta3 integrin in ovarian cancer. Neoplasia. 2008; 10:1259–1267. [PubMed: 18953435]
20. Halder J, Kamat AA, Landen CN Jr, Han LY, Lutgendorf SK, Lin YG, et al. Focal adhesion kinase targeting using in vivo short interfering RNA delivery in neutral liposomes for ovarian carcinoma therapy. Clin Cancer Res. 2006; 12:4916–4924. [PubMed: 16914580]
21. Buick RN, Pullano R, Trent JM. Comparative properties of five human ovarian adenocarcinoma cell lines. Cancer Res. 1985; 45:3668–3676. [PubMed: 4016745]
22. Moore DH, Allison B, Look KY, Sutton GP, Bigsby RM. Collagenase expression in ovarian cancer cell lines. Gynecol Oncol. 1997; 65:78–82. [PubMed: 9103395]
23. Yu D, Wolf JK, Scanlon M, Price JE, Hung MC. Enhanced c-erbB-2/neu expression in human ovarian cancer cells correlates with more severe malignancy that can be suppressed by E1A. Cancer Res. 1993; 53:891–898. [PubMed: 8094034]
24. Duan Z, Feller AJ, Toh HC, Makastorsis T, Seiden MV. TRAG-3, a novel gene, isolated from a taxol-resistant ovarian carcinoma cell line. Gene. 1999; 229:75–81. [PubMed: 10095106]
25. Landen CN Jr, Lu C, Han LY, Coffman KT, Bruckheimer E, Halder J, et al. Efficacy and antivascular effects of EphA2 reduction with an agonistic antibody in ovarian cancer. J Natl Cancer Inst. 2006; 98:1558–1570. [PubMed: 17077358]
26. Steg A, Wang W, Blanquicett C, Grunda JM, Eltoum IA, Wang K, et al. Multiple gene expression analyses in paraffin-embedded tissues by TaqMan low-density array: Application to hedgehog and Wnt pathway analysis in ovarian endometrioid adenocarcinoma. J Mol Diagn. 2006; 8:76–83. [PubMed: 16436637]
27. Landen CN Jr, Goodman B, Katre AA, Steg AD, Nick AM, Stone RL, et al. Targeting aldehyde dehydrogenase cancer stem cells in ovarian cancer. Mol Cancer Ther. 2010; 9:3186–3199. [PubMed: 20889728]
28. Kavallaris M. Microtubules and resistance to tubulin-binding agents. Nat Rev Cancer. 2010; 10:194–204. [PubMed: 20147901]

29. Steg AD, Bevis KS, Katre AA, Ziebarth A, Dobbin ZC, Alvarez RD, et al. Stem cell pathways contribute to clinical chemoresistance in ovarian cancer. Clin Cancer Res. 2012; 18:869–881. [PubMed: 22142828]

30. Silva IA, Bai S, McLean K, Yang K, Griffith K, Thomas D, et al. Aldehyde dehydrogenase in combination with CD133 defines angiogenic ovarian cancer stem cells that portend poor patient survival. Cancer Res. 2011; 71:3991–4001. [PubMed: 21498635]

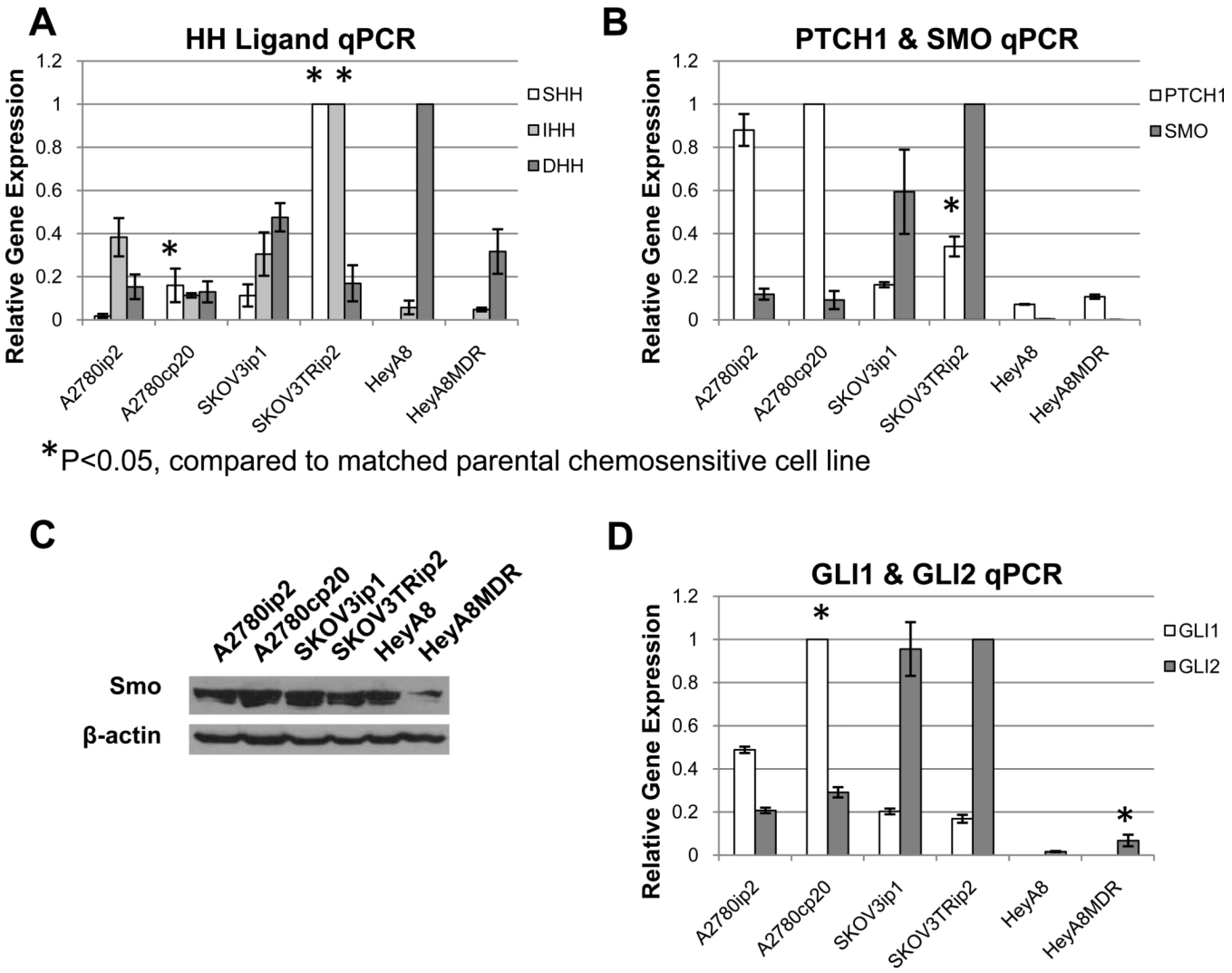

Figure 1. Expression of HH signaling comoponents in chemosensitive and chemoresistant ovarian cancer cell lines

Gene expression was calculated relative to the sample/cell line with the highest expression of a particular gene. A) mRNA expression of HH ligands, Sonic (*SHH*), Indian (*IHH*) and Desert (*DHH*). B) mRNA expression of HH receptors, *PTCH1* and *SMO*. C) Protein expression of Smo was also measured using Western blot analysis. β-actin was used as a loading control. D) mRNA expression of HH transcription factors, *GLI1* and *GLI2*. Data are representative of 3 independent experiments. **P* < 0.05, compared to parental chemosensitive cell line.

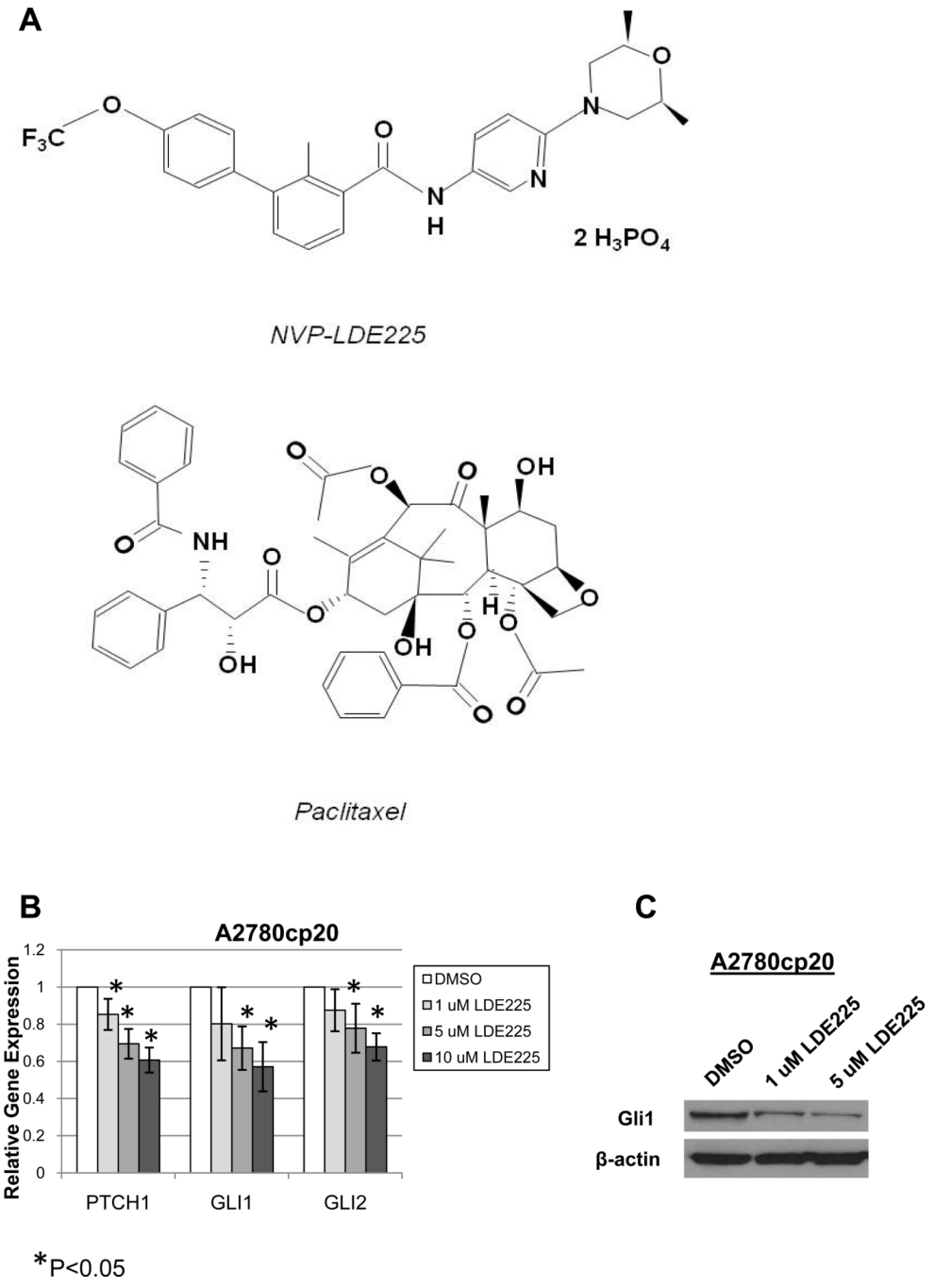

Figure 2. LDE225 reduces HH pathway activity in chemoresistant ovarian cancer cells

A) Chemical structures of NVP-LDE225 and paclitaxel. B) Gene expression of *PTCH1*, *GLI1* and *GLI2* was examined in A2780cp20 cells following exposure to increasing concentrations of LDE225 using qPCR. **P* < 0.05, compared to DMSO vehicle control. C) Protein expression of Gli1 in A2780cp20 cells following exposure to increasing concentrations of LDE225 was measured using Western blot analysis to confirm mRNA results. β-actin was used as a loading control. Data are representative of 3 independent experiments.

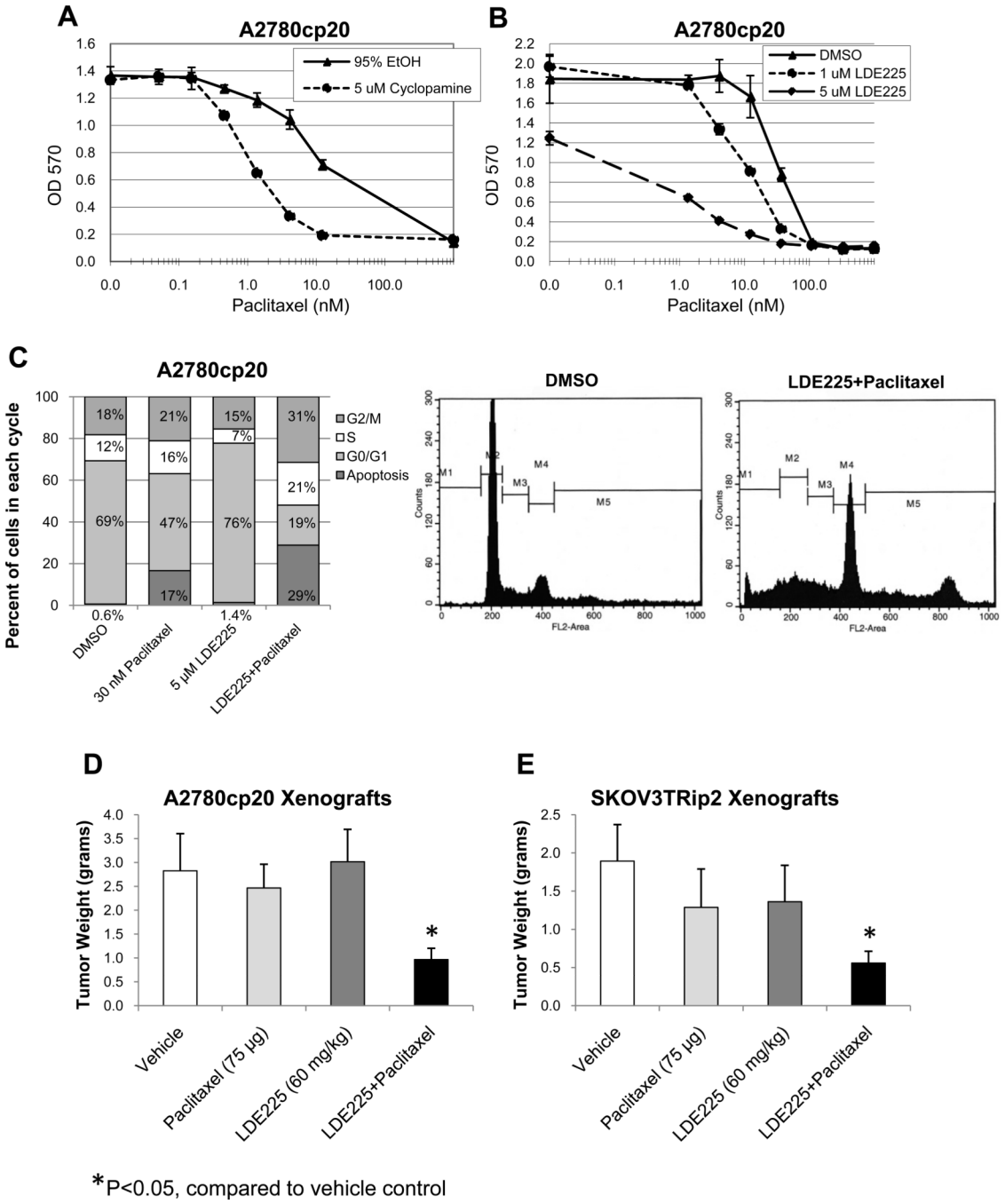

Figure 3. Smo antagonism reverses taxane resistance in chemoresistant ovarian cancer cell lines both *in vitro* and *in vivo*

A) A2780cp20 cells were exposed to either 95% ethanol (EtOH, vehicle control) or cyclopamine (5 μM) in combination with increasing concentrations of paclitaxel. Cell viability was determined by MTT assay. B) A2780cp20 cells were exposed to either DMSO (vehicle control) or LDE225 (1 and 5 μM) in combination with increasing concentrations of paclitaxel. Cell viability was determined by MTT assay. C) Cell cycle analysis was performed on A2780cp20 cells treated with DMSO alone, paclitaxel alone, LDE225 alone or combined paclitaxel and LDE225 using propidium iodide (PI) staining. Representative histograms of DMSO- and combination-treated cells are shown on the right. Data are

representative of 3 independent experiments. D) Mice injected intraperitoneally with A2780cp20 cells were treated with either vehicle alone, paclitaxel alone, LDE225 alone or combined paclitaxel + LDE225. E) Mice injected intraperitoneally with SKOV3TRip2 cells were treated with either vehicle alone, paclitaxel alone, LDE225 alone or combined paclitaxel + LDE225. For both xenograft models, mice treated with the combination paclitaxel + LDE225 showed a significant reduction in tumor weight compared to treatment with vehicle alone. Mean tumor weights with standard error are presented. $*P < 0.05$, compared to vehicle control.

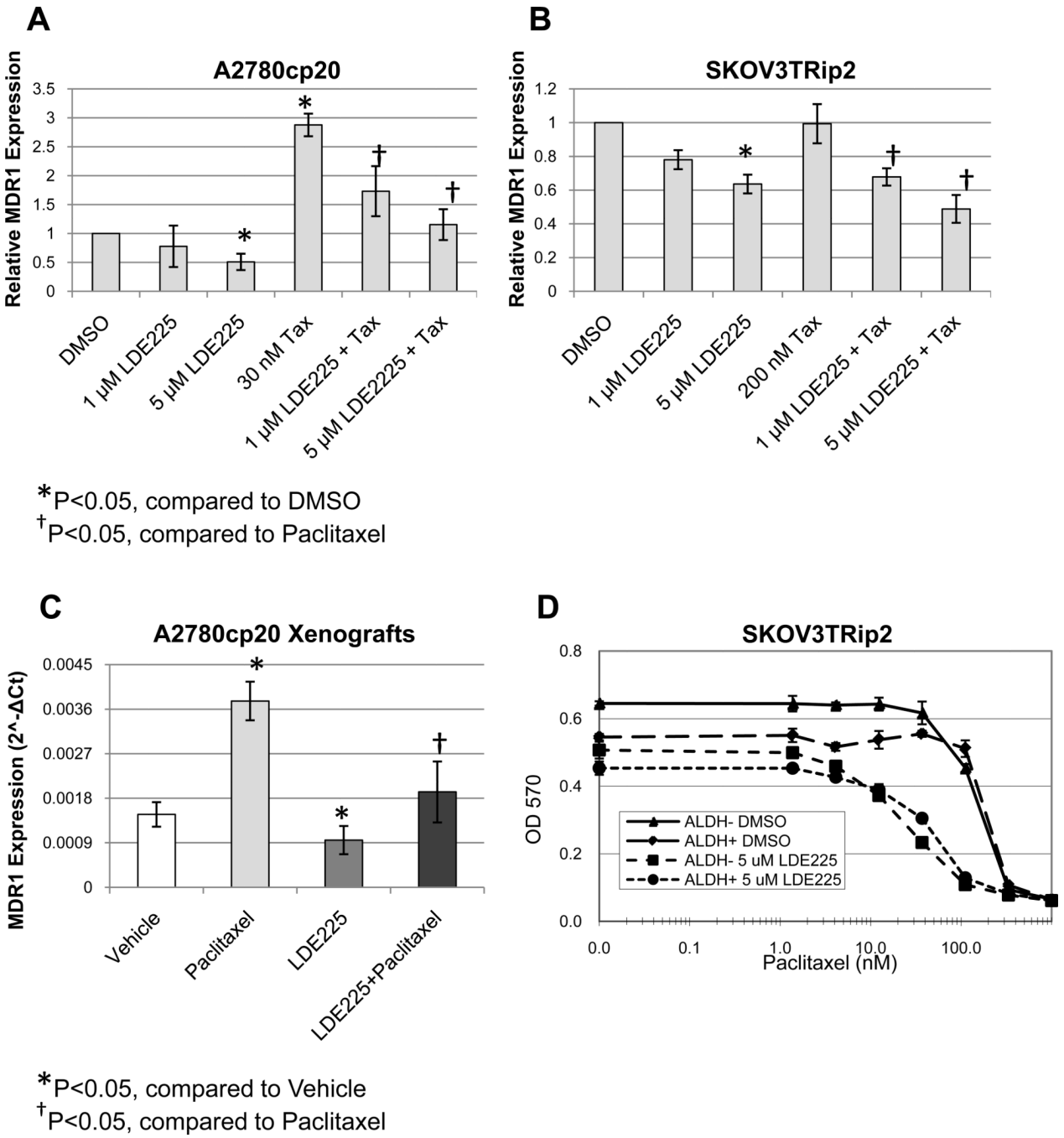

Figure 4. LDE225 sensitizes chemoresistant ovarian cancer cells to paclitaxel by downregulating MDR1 expression and sensitizes both ALDH-negative and -positive ovarian cancer cells to paclitaxel

A) A2780cp20 cells were exposed to DMSO, LDE225 (1 or 5 μM), paclitaxel (Tax, 30 nM) or combined LDE225 + paclitaxel for 72 hours and examined for *MDR1* gene expression. **P* < 0.05, compared to DMSO; †*P* < 0.05, compared to paclitaxel alone. B) SKOV3TRip2 cells were exposed to DMSO, LDE225 (1 or 5 μM), paclitaxel (Tax, 200 nM) or combined LDE225 + paclitaxel for 72 hours and examined for *MDR1* gene expression. **P* < 0.05, compared to DMSO; †*P* < 0.05, compared to paclitaxel alone. Data are representative of 3 independent experiments. C) A2780cp20 xenografts (n = 5 per group) treated with vehicle

alone, paclitaxel alone, LDE225 alone or combined LDE225 + paclitaxel were resected after 4 weeks of therapy and examined for *MDR1* gene expression. Mean expression with standard error are presented. *$P < 0.05$, compared to vehicle; †$P < 0.05$, compared to paclitaxel alone. D) SKOV3TRip2 cells were sorted into aldehyde dehydrogenase-negative (ALDH−) and -positive (ALDH+) populations, using the ALDEFLUOR assay, and then exposed to either DMSO or 5 μM LDE225, both alone and in combination with increasing concentrations of paclitaxel. Cell viability was determined by MTT assay.

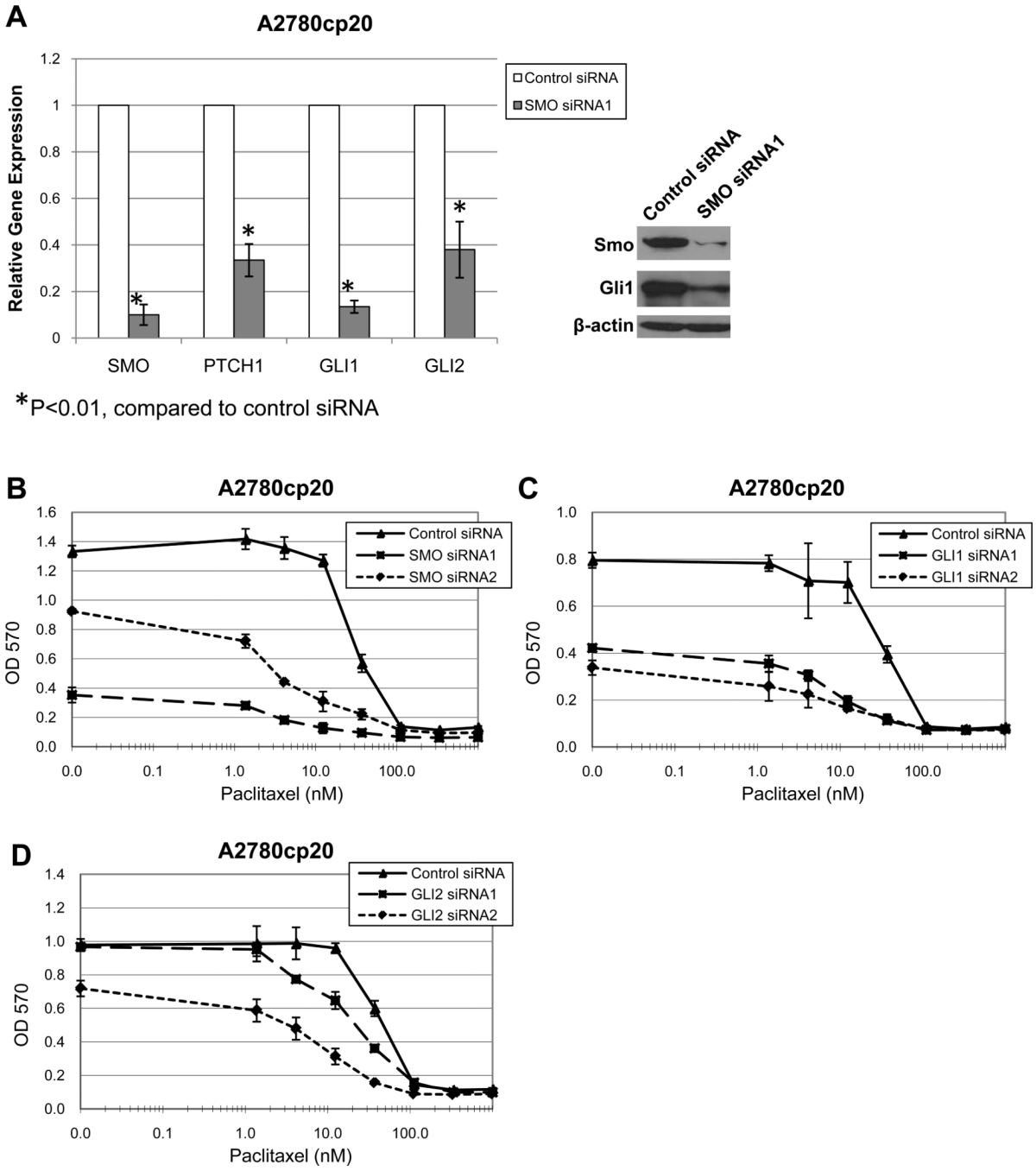

Figure 5. Knockdown of Smo diminishes HH pathway activity, reduces viability and reverses taxane resistance in ovarian cancer cells

A) A2780cp20 cells were exposed to either control or Smo siRNA for 72 hours and examined for mRNA expression of HH pathway mediators *SMO*, *PTCH1*, *GLI1* and *GLI2*. **P* < 0.01, compared to control siRNA. Protein expression of Smo and Gli (inset) was also measured using Western blot analysis to confirm mRNA results. β-actin was used as a loading control. A2780cp20 cells were transfected with either control siRNA or 2 distinct siRNA constructs designed against Smo (B), Gli1 (C) or Gli2 (D) and exposed to increasing concentrations of paclitaxel. Cell viability was determined by MTT assay. Data are representative of 3 independent experiments.

Table 1

Ovarian cancer cell line response to Smo antagonists, alone and in combination with paclitaxel

	Mean IC50			Mean Paclitaxel IC50		
Cell Line	**Cyclopamine**	**LDE225**	**Control**	**w/Cyclopamine (5 uM)**	**w/LDE225 (5 uM)**	***p* -value**
A2780ip2	7.5 μM	12 μM	4 nM	1.5 nM	2.6 nM	NS
A2780cp20	10 μM	7.5 μM	30 nM	1.3 nM	1.5 nM	<0.05
SKOV3ip1	14 μM	24 μM	6 nM	3 nM	5.5 nM	NS
SKOV3TRip2	19 μM	12 μM	400 nM	15 nM	120 nM	<0.05
HeyA8	12 μM	18 μM	7 nM	4.2 nM	6.5 nM	NS
HeyA8MDR	13 μM	8 μM	650 nM	50 nM	115 nM	<0.05